

SHAPE SENSITIVITY ANALYSIS INCLUDING QUALITY CONTROL WITH CARTESIAN FINITE ELEMENT MESHES

J.J. RÓDENAS, J.E. TARANCÓN, O. MARCO AND E. NADAL

Centro de Investigación de Tecnología de Vehículos (CITV)
Universitat Politècnica de València, Camino de Vera, s/n, E-46022 Valencia, Spain
e-mail: {jjrodena,jetaranc}@mcm.upv.es {onmaral,ennaso}@upvnet.upv.es

Key words: Cartesian Grid-FEM, NURBS, velocity field, shape sensitivity analysis

Abstract. The gradient-based optimization methods used for optimization of structural components require that the information of the gradients (sensitivity) of the magnitudes of interest with respect to the design variables is calculated with sufficient accuracy. The aim of this paper is to present a module for calculation of shape sensitivities with geometric representation by NURBS (Non-Uniform Rational B-Splines) for a program created to analyze 2-D linear elasticity problems, solved by FEM using cartesian grids independent of the geometry, CG-FEM.

First, it has been implemented the ability to define the geometry using NURBS, which have become in recent years in the most used geometric technology in the field of engineering design. In order to be able to represent exact geometries, a scheme based on matrix representation of this type of curve and proper integration is proposed. Moreover, the procedures for shape sensitivities calculation, for standard FEM, have been adapted to an environment based on cartesian meshes independent of geometry, which implies, for instance, a special treatment of the elements trimmed by the boundary and the implementation of new efficient methods of velocity field generation, which is a crucial step in this kind of analysis.

Secondly, an error estimator, as an extension of the error estimator in energy norm developed by Zienkiewicz and Zhu, has been proposed for its application to the estimation of the discretization error arising from shape sensitivity analysis in the context of cartesian grids.

The results will show how using NURBS curves involves significant decrease of geometrical error during FE calculation, and that the calculation module implemented is able to efficiently provide accurate results in sensitivity analysis thanks to the use of the CG-FEM technology.

1 INTRODUCTION

This paper presents an approach for calculation of shape sensitivities based on the use of cartesian meshes independent of the geometry. Gradient based optimization processes require this kind of information, and its accuracy influences the evolution of the process. Specifically, this paper focuses on 2-D optimization problems, with exact representation of the geometries, governed by the linear elasticity equations, using FEM to determine the sensitivity of the quantities of interest.

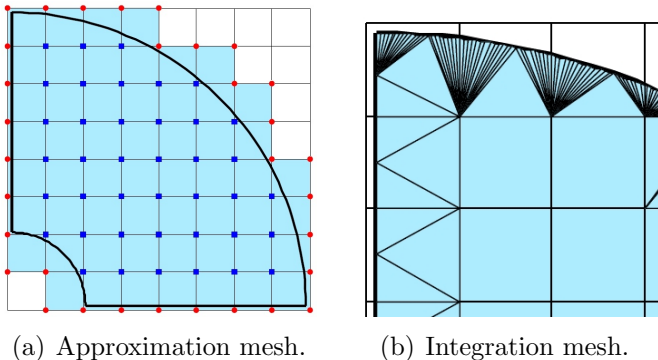


Figure 1: Example of meshes related to CG-FEM.

Meshes independent of the geometry are used as a tool to alleviate the meshing and remeshing burden, for example, in the Generalized FEM (GFEM)[1] or Extended FEM (XFEM)[2]. The analysis procedure makes use of two meshes, an approximation mesh, which is a mesh that covers the original domain and is used for the construction of the approximation basis, and an integration mesh intended for numerical evaluation of all integrals.

The approximation mesh needs to be a FE mesh satisfying only the requirement of covering completely the problem extension, as shown in Fig. 1(a), while the integration mesh is obtained by the division into subdomains of each element of the approximation mesh separately, taking into account the local geometry of the domain as shown in Fig. 1(b). For this subdivision the Delaunay triangulation is used, generating integration subdomains whose number will depend on the curvature of the edge crossing the elements.

In addition to this, the elements are disposed following a cartesian grid pattern in order to achieve significant computational savings, absolutely necessary in optimization analysis, where iterative analyses leading to considerable data flows are required.

Nowadays engineering analysis and high-performance computing are also demanding greater precision and tighter integration of the overall modeling-analysis process. In this regard, we will reduce errors by focusing on one, and only one, geometric model, which can be utilized directly as an analysis model. There are a number of candidate computational geometry technologies that may be used. The most widely used in engineering design are NURBS (Non-Uniform Rational B-splines), the industry standard. NURBS are convenient for free-form surface modeling, can exactly represent conic sections such as circles, cylinders, spheres, etc., and there exist many efficient and numerically stable algorithms to generate them. In order to achieve an accurate geometrical representation we present in this paper a combination of exact geometrical modeling, using NURBS

technology, and proper numerical integration while maintaining standard polynomial FE interpolation (isoparametric formulation).

Some of the most popular optimization methods are the gradient-based methods, based on the calculation of derivatives (sensitivities). To evaluate these gradients, a sensitivity analysis with respect to design variables is necessary. The design variables are defined by the analyst and describe the geometry of the component to be optimized. As a prelude to the calculation of sensitivities, it is necessary to define how to vary the position of material points of the domain in relation to the design variables, i.e. the sensitivity of the coordinates of the particles. This sensitivity can be interpreted as a velocity field, and its quality will affect the accuracy of the results. In this work we adapt the calculation of sensitivities to an CG-FEM environment, dribbling the problems arising from the use of meshes independent of the geometry and taking advantage of the cartesian grid structure. To evaluate the quality of the calculations we will implement an error estimator based on SPR techniques.

2 EXACT GEOMETRICAL REPRESENTATION

This section gives a brief introduction to NURBS[3][4]. In addition, it explains practical features when operating with cartesian meshes. A NURBS curve is defined as follows

$$P(t) = \frac{\sum_{i=0}^n N_{i,p}(t) w_i B_i}{\sum_{i=0}^n N_{i,p}(t) w_i} \quad 0 \leq t \leq 1 \quad (1)$$

where $B_i = (x_i, y_i)$ represents the coordinate positions of a set of $i = 0, \dots, n$ control points, w_i is the corresponding weight, and $N_{i,p}$ is the degree p B-spline basis function defined on the knot vector

$$K_t = \{t_0, t_1, \dots, t_{n+p+1}\} \quad (2)$$

The i -th ($i = 0, \dots, n$) B-spline basis function can be defined recursively as

$$N_{i,p}(t) = \frac{(t - t_i) N_{i,p-1}(t)}{t_{i+p} - t_i} + \frac{(t_{i+p+1} - t) N_{i+1,p-1}(t)}{t_{i+p+1} - t_{i+1}} \quad N_{i,0}(t) = \begin{cases} 1 & t_i \leq t \leq t_{i+1} \\ 0 & \text{otherwise} \end{cases} \quad (3)$$

The polynomial space spanned by the B-spline basis can be converted into the piecewise polynomial representation spanned by the power basis so that the matrix representation for B-spline curves is always possible. There are some situations where it may be advantageous to generate the coefficients of each of the polynomial pieces, e.g., when we have to evaluate the curve at a large number of points or when we have to intersect the geometry with the mesh, as we will see later. Explicit matrix forms we have used would make it easier and faster because polynomial evaluation is more efficient in a power basis. In this work we have used a recursive procedure to get these matrices[5], then if we can represent

each section of the NURBS by standard parameter $u = \frac{t-t_i}{t_{i+1}-t_i}$ being $t \in [t_i, t_{i+1})$ the range that defines each one of them, we can write the matrix representation of a NURBS as

$$P(j, u) = \frac{U(u)M(j)w(j)B(j)}{U(u)M(j)w(j)} \quad (4)$$

where $U = \{1 \ u \ u^2 \dots \ u^p\}$, $M(j)$ the coefficient matrix corresponding to the span j , $B(j)$ the coordinates of the control points that influence the span j and $h(j)$ the weights for these control points.

One of the major tasks observed by using cartesian meshes independent of the geometry is the evaluation of its intersection with the geometric entities. Although the mesh is formed only by straight lines, the task of processing the intersections is a great computational effort. Although NURBS are rational curves, intersecting with straight lines implies that we can transform the NURBS rational expression in a non-rational polynomial expression, and therefore any algorithm to find polynomial roots will be valid.

As seen in Fig. 1(b) the integration mesh is composed by the internal elements and the subdomains created using a Delaunay triangulation depending on the curvature of the boundary. This triangulation attempts to capture the curvature of the geometry in order to solve the numerical integrals. However a linear triangulation, as in Fig. 1(b), will not suffice if we want to take advantage of exact geometries, so we use a coordinate transformation that allows us to accurately represent the problem domain. To achieve this the *transfinite interpolation*[6], commonly used in p -adaptivity, is ideal because it performs a mapping using area coordinates of triangles to locate the integration points considering the exact geometry, this computational effort will be located only in the boundary elements which reduces the number of triangular mappings to be done.

3 SHAPE SENSITIVITY ANALYSIS

In this paper we solve 2-D elasticity problems where discrete equilibrium equation is

$$\mathbf{K}\mathbf{u} = \mathbf{f} \quad (5)$$

and its derivative with respect to any design variable a_m is given by

$$\frac{\partial \mathbf{K}}{\partial a_m} \mathbf{u} + \mathbf{K} \frac{\partial \mathbf{u}}{\partial a_m} = \frac{\partial \mathbf{f}}{\partial a_m} \quad \text{and rearranging} \quad \mathbf{K} \frac{\partial \mathbf{u}}{\partial a_m} = \frac{\partial \mathbf{f}}{\partial a_m} - \frac{\partial \mathbf{K}}{\partial a_m} \mathbf{u} \quad (6)$$

where \mathbf{K} and $\frac{\partial \mathbf{K}}{\partial a_m}$ are the global stiffness and stiffness sensitivity matrices and $\frac{\partial \mathbf{f}}{\partial a_m}$ are the equivalent forces sensitivities, considered null value because it is assumed that the applied forces will not change with the introduction of a disturbance of differential order.

Let us consider the formulation of isoparametric 2-D elements. The stiffness matrix of the element is given by

$$\mathbf{k}^e = \int_{\Omega^e} \mathbf{B}^T \mathbf{D} \mathbf{B} |J| d\Omega \quad (7)$$

where Ω^e is the domain in local element coordinates, \mathbf{B} is the nodal strains-displacements matrix, \mathbf{D} is the stiffness matrix that relates stresses with strains and $|\mathbf{J}|$ is the determinant of the Jacobian matrix.

Considering the derivative of \mathbf{D} with respect to design variables is zero we will have

$$\frac{\partial \mathbf{k}^e}{\partial a_m} = \int_{\Omega^e} \left[\frac{\partial \mathbf{B}^T}{\partial a_m} \mathbf{D} \mathbf{B} + \mathbf{B}^T \mathbf{D} \frac{\partial \mathbf{B}}{\partial a_m} \right] |\mathbf{J}| d\Omega + \int_{\Omega^e} \left[\mathbf{B}^T \mathbf{D} \mathbf{B} \frac{\partial |\mathbf{J}|}{\partial a_m} \right] d\Omega \quad (8)$$

where all members can be evaluated numerically, although the calculation of $\frac{\partial \mathbf{B}}{\partial a_m}$ and $\frac{\partial |\mathbf{J}|}{\partial a_m}$ will require the sensitivity of the nodal coordinates, known as velocity field, defined as

$$\frac{\partial}{\partial a_m} \{x_i, y_i\} = \mathbf{V}_m(x_i, y_i) \quad (9)$$

The velocity field along the contour can be easily evaluated from the parametric description of the boundary. Theoretically, the velocity field is subject to only two requirements: regularity and linear dependency[7] with respect to the design variables.

To ensure the quality of the velocity field is even more important when using cartesian meshes independent of the geometry, since the integration mesh has elements intersected with the boundary, leading to internal and external nodes (blue squares and red circles respectively in Fig. 1(a)) needed to be assigned an appropriate velocity field satisfying the boundary conditions imposed.

From now on we will use the problem of a 1/4 of cylinder under internal pressure (Figs. 2(a) and 2(b)), to illustrate the velocity field generation process. In the sensitivity analysis of this example is considered only one design variable corresponding to the outer radius of the cylinder, thus taking $a_m = b$. The strategy will be to impose a velocity field on the boundary evaluated (Fig. 2(c)), for instance, using a finite difference scheme, and then to perform an interpolation to the rest of the internal domain and an extrapolation to the external nodes; so we present the next alternatives:

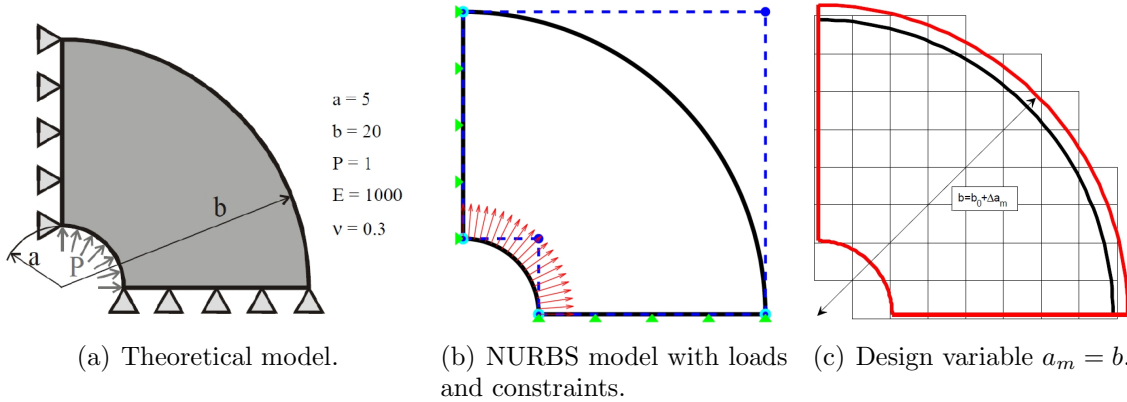


Figure 2: Cylinder under internal pressure. Problem definition.

Complete domain velocity field. This option implies to interpolate by picking points over the boundary and weighting the inverse of their distance with respect every internal node. For the external nodes, knowing the information in the boundary and in the internal domain it is possible to fit local polynomial surfaces on patches of elements around these nodes in order to get a proper extrapolation of the information. An output for the example is Fig. 3(a).

Contour adjacent elements velocity field. Knowing that any velocity field, satisfying some conditions, would be suitable for calculation of sensitivities, at least theoretically, we could obviate the internal domain and follow the previous strategy but only in the elements intersected with the boundary. This would lead to important computational savings without sacrificing much accuracy. See Fig. 3(b).

Physical approach. We can set up a load case where the Dirichlet boundary conditions are a velocity field[8], then, solving a FEM problem, we could obtain a solution that represents a velocity field on all active nodes. This solution will be very smooth but with the computational cost related to solving a system of equation. See Fig. 3(c). Note that iterative solvers can be used to solve the system of equations. If the intermediate solutions satisfy Dirichlet boundary conditions then they can be used as velocity fields as they meet the theoretical requirements thus reducing the computational cost to obtain a valid velocity field.

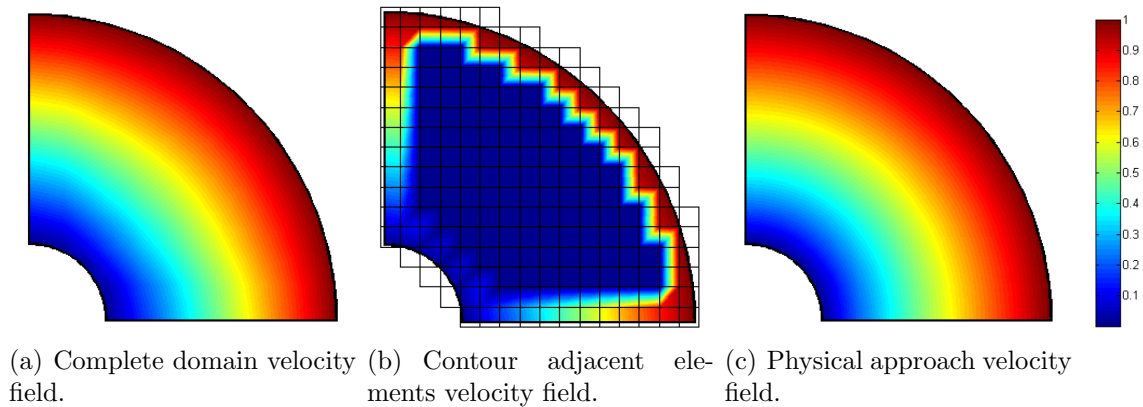


Figure 3: Comparison between different velocity fields for the cylinder example.

4 ERROR ESTIMATION BASED ON RECOVERY TECHNIQUES

In general it is not possible to know the exact error of the solution associated to the FE discretization in the problem analyzed, since this requires knowing the exact solution of the problem. Currently different methods have been developed to estimate the discretization error of the FE solution.

For linear elasticity problems the energy norm $\|\mathbf{u}\|$ is commonly used for quantifying the discretization error of the solution obtained from the FE analysis. In order to evaluate an estimate, $\|\mathbf{e}_{es}\|$, of the exact value of the discretization error in energy norm, $\|\mathbf{e}_{ex}\|$, Zienkiewicz and Zhu[9] developed the *ZZ estimator*, which is currently in wide use, proposing the use of the following expression:

$$\|\mathbf{e}_{es}\|^2 = \int_{\Omega} (\boldsymbol{\sigma}^* - \boldsymbol{\sigma}^h)^T \mathbf{D}^{-1} (\boldsymbol{\sigma}^* - \boldsymbol{\sigma}^h) d\Omega \quad (10)$$

where domain Ω can refer to either the whole domain or a local (element) subdomain, $\boldsymbol{\sigma}^h$ represents the stresses evaluated using the FE method, $\boldsymbol{\sigma}^*$ is the so called smoothed or recovered stress field, that is a better approximation to the exact solution than the FE stresses $\boldsymbol{\sigma}^h$. In defining the $\boldsymbol{\sigma}^*$ field inside of each element the following expression is normally used:

$$\boldsymbol{\sigma}^* = \mathbf{N} \underline{\boldsymbol{\sigma}}^* \quad (11)$$

where \mathbf{N} are the same shape functions used in the interpolation of the FE displacements field and $\underline{\boldsymbol{\sigma}}^*$ is the vector of smoothed nodal stresses in the element.

4.1 The SPR Technique and its Modifications

It becomes evident from (10) and (11) that the precision of the ZZ estimator will be a function of the smoothing technique used to obtain the nodal values $\underline{\boldsymbol{\sigma}}^*$. Because of its accuracy, robustness, simplicity and low computational cost, one of the most popular techniques used to evaluate $\underline{\boldsymbol{\sigma}}^*$ is the *Superconvergent Patch Recovery* (SPR) technique developed by Zienkiewicz and Zhu[10].

The components of $\underline{\boldsymbol{\sigma}}^*$ are obtained from a polynomial expansion, σ_p^* , defined over a set of contiguous elements called patch which consists of all of the elements sharing a vertex node, of the same complete order q as that of the shape functions \mathbf{N} . For each of the stress components of this polynomial, σ_p^* is found using the following expression:

$$\sigma_p^* = \mathbf{p} \mathbf{a} \quad (12)$$

where \mathbf{p} contains the terms of the polynomial and \mathbf{a} is the vector of polynomial unknown coefficients.

The data of the FE stresses calculated at the superconvergence points are used to evaluate \mathbf{a} by means of a least-square fit. Once the \mathbf{a} parameters have been calculated for each stress component, the values of $\underline{\boldsymbol{\sigma}}^*$ are obtained by substituting the nodal coordinates into the polynomial expressions σ_p^* .

After the publication of the SPR technique, a great number of articles followed which proposed modifications generally based on an approximate satisfaction of equilibrium equations to improve its performance. In this paper we will use an implementation of the SPR-C technique[11] which is a modification of the original SPR technique with the

objective of improving the values of $\underline{\sigma}^*$. In this approach constraint equations are applied over the \mathbf{a} coefficients that define the stress interpolation polynomials in the patch σ_p^* , so that these polynomials can satisfy both field equations (internal equilibrium equation and compatibility equation) and boundary conditions (boundary equilibrium equation, symmetry boundary condition, etc.) as far as the representation of σ^* by means of polynomials can allow. The constraint equations over the \mathbf{a} coefficients are applied using the Lagrange's multipliers method.

4.2 Error Estimation in Sensitivities

As explained before, the sensitivity of the FE solution will not be exact, regardless of the method used for calculating sensitivities. So we will need to determine a magnitude to quantify the discretization error in sensitivities associated to the FE discretization.

Following [12], we will use the sensitivity of the square of the energy norm with respect to the design variable considered as magnitude for the quantification of the discretization error in sensitivities. This sensitivity is defined as the variation of the square of the energy norm with respect to the design variables, i.e.:

$$\chi_m = \frac{\partial \|\mathbf{u}\|^2}{\partial a_m} = \sum \int_{\Omega^e} \boldsymbol{\sigma}^T \mathbf{D}^{-1} \left(2 \left(\frac{\partial \boldsymbol{\sigma}}{\partial a_m} \right) + \frac{\boldsymbol{\sigma}}{|\mathbf{J}|} \frac{\partial |\mathbf{J}|}{\partial a_m} \right) |\mathbf{J}| d\Omega^e \quad (13)$$

The discretization error in sensitivities can be evaluated deriving (10) with respect to the design variables, yielding

$$e(\chi_m)_{es} = \sum \int_{\Omega^e} \left((\boldsymbol{\sigma}^* - \boldsymbol{\sigma}^h)^T \mathbf{D}^{-1} \left(2 \left[\left(\frac{\partial \boldsymbol{\sigma}}{\partial a_m} \right)^* - \frac{\partial \boldsymbol{\sigma}^h}{\partial a_m} \right] + \frac{(\boldsymbol{\sigma}^* - \boldsymbol{\sigma}^h)}{|\mathbf{J}|} \frac{\partial |\mathbf{J}|}{\partial a_m} \right) |\mathbf{J}| \right) d\Omega^e \quad (14)$$

where, considering $\underline{\mathbf{u}}^e$ as displacements at nodes of each element e , $\frac{\partial \boldsymbol{\sigma}^h}{\partial a_m}$ is given by:

$$\frac{\partial \boldsymbol{\sigma}^h}{\partial a_m} = \mathbf{D} \mathbf{B} \frac{\partial \underline{\mathbf{u}}^e}{\partial a_m} + \mathbf{D} \frac{\partial \mathbf{D}}{\partial a_m} \underline{\mathbf{u}}^e \quad (15)$$

In addition it is important to point out that in order to smoothing the derivatives of the stress field with respect to the design variables $\left(\frac{\partial \boldsymbol{\sigma}}{\partial a_m} \right)^*$, we will apply recovery techniques similar to those used with the stress field $\boldsymbol{\sigma}^*$.

The computational cost will be reduced since it only requires the determination of $\left(\frac{\partial \boldsymbol{\sigma}}{\partial a_m} \right)^*$ and the direct application of the above equation. The remaining quantities involved in the above expression ($|\mathbf{J}|$, $\frac{\partial |\mathbf{J}|}{\partial a_m}$ and $\boldsymbol{\sigma}^*$) will be available through previous calculations of the analysis, the calculation of sensitivities and the estimation of the discretization error in energy norm. We have to say that the smoothing of the stress field will be carried out with the SPR-C technique while the field of stress derivatives will be recovered with the standard SPR technique.

5 NUMERICAL RESULTS

Before starting with numerical comparisons we have to define some magnitudes to help us to evaluate and to understand the results obtained. First of all, we define the estimated relative error in sensitivities. This is more easily interpretable than the absolute error, then we will have

$$\eta(\chi_m)_{es} = \sqrt{\left| \frac{e(\chi_m)_{es}}{\chi_m + e(\chi_m)_{es}} \right|} \quad (16)$$

To evaluate the effectivity of the error estimator in sensitivities we will use

$$\theta(\chi_m) = \sqrt{\left| \frac{e(\chi_m)_{es}}{e(\chi_m)_{ex}} \right|} \quad (17)$$

In addition, we can find in [12] a relationship between the discretization error in energy norm and the discretization error in sensitivities. This relationship between the two types of errors can be used as an indicator quality of the results obtained from the velocity field generation process, being defined as

$$\frac{e(\chi_m)_{ex}}{\|e(\mathbf{u})_{ex}\|^2} \approx const. \quad (18)$$

Now we will show the analyses performed to evaluate the proper behavior of the work developed and the accuracy of the results. For proper evaluation of the results we will evaluate the parameters defined in the previous paragraphs.

The exact solution for the problem defined in Fig.2 is: energy norm $\|\mathbf{u}_{ex}\|^2 = 2\Pi = 0.055815629478779$ and $\chi_{m_{ex}} = -5.082398781807488 \cdot 10^{-4}$.

For this problem we will compare the complete domain velocity field, the contour adjacent elements velocity field and a velocity field calculated by the physical approach of FE. Also we will use a field imposed analytically so that we can judge the goodness of the methods developed. This field is calculated directly at nodes following the expression $\mathbf{V}_m = (r \cdot A - B) \cdot \Delta a_m$ where the coefficients A and B will define a growing linear function from the axis of the cylinder depending on the nodal distance r .

The first analysis will be an h -adaptive refinement procedure with linear elements to observe the performance differences between inner and outer arcs created with NURBS or with standard splines defined with with different sets of interpolation points, 3 to 9.

In Figs. 4(a) and 4(c), we can evaluate the results in magnitudes related to the sensitivity analysis, where we can see that the convergence rate and the quality constant are better in the geometry defined by NURBS. But Fig. 4(b) is very important as it shows the error in energy norm and we see how for splines the convergence rate tends to zero as it approaches a value of error, related with the geometrical definition error, while for the geometry defined by NURBS the value of the error continues decreasing steadily.

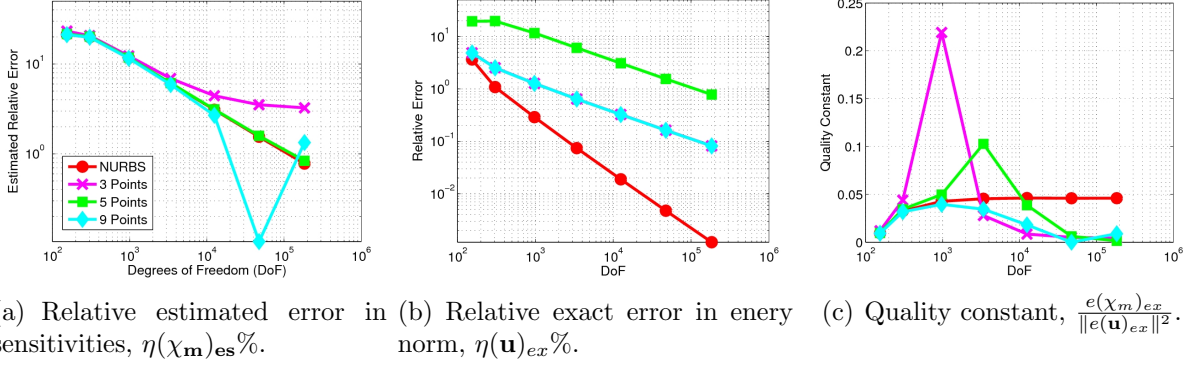


Figure 4: Effect of using NURBS. h -adaptive refinement and analytical velocity field.

After seeing these results, the remaining analyses in this section will use NURBS geometry. The simulations will be two analyses with linear elements and mesh refinement, one with uniform refinement and the other with h -adapted meshes. Both will compare the analytical velocity field and the one obtained by the physical approach of FE, with the complete domain velocity field and the contour adjacent elements velocity field.

Regarding uniform refinement, Fig. 5(a) shows similar convergence rate for the latest meshes, but when comparing the quality constant and the effectivity, in Figs. 5(b) and 5(c), only the field generated by the physical approach is able to match convergence rate and to maintain quality constant stable with respect the analytically imposed.

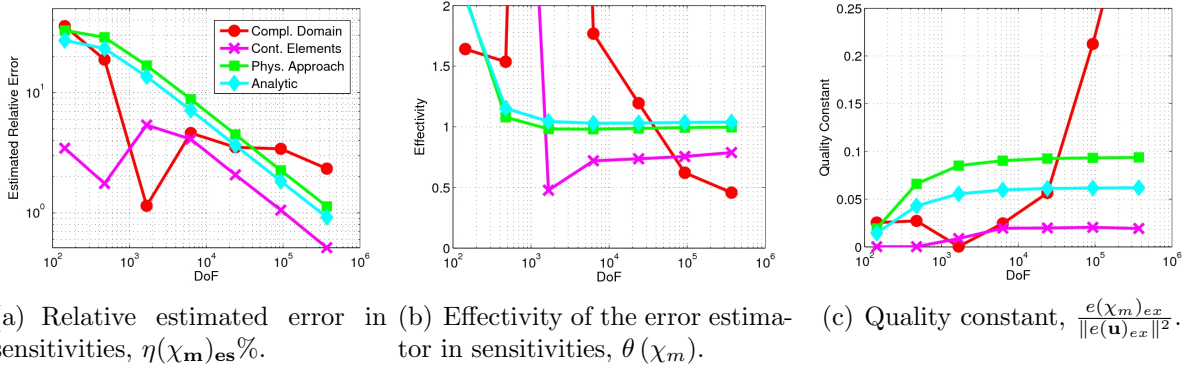
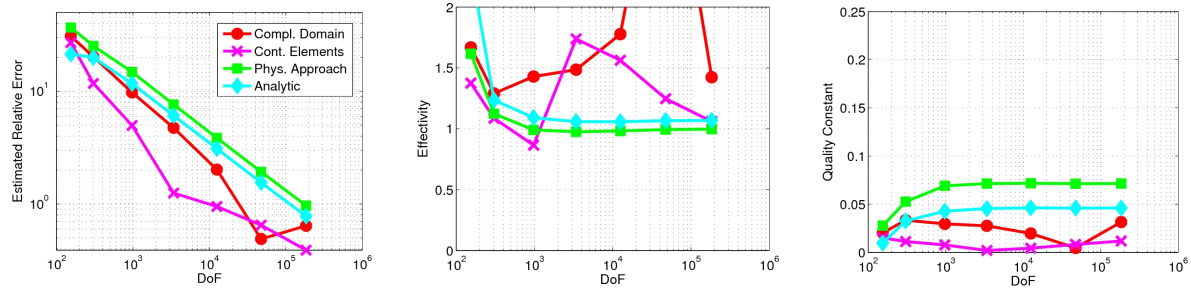


Figure 5: Effect of velocity field. Uniform refinement. Geometry defined by NURBS.

If we use h -adaptive meshes then we will get similar results. The value of the convergence rate is good overall, (Fig. 6(a)). The effectivity index of the physical approach is the only capable of keeping up with the analytical velocity field, Fig. 6(b), but the quality constant of the velocity fields is acceptable for all of them, Fig. 6(c).



(a) Relative estimated error in sensitivities, $\eta(\chi_m)_{es}\%$. (b) Effectivity of the error estimator in sensitivities, $\theta(\chi_m)$. (c) Quality constant, $\frac{e(\chi_m)_{ex}}{\|e(\mathbf{u})_{ex}\|^2}$.

Figure 6: Effect of velocity field. h -adaptive refinement. Geometry defined by NURBS.

6 CONCLUSIONS

This paper presents a module for the calculation of shape sensitivities with geometric representation by NURBS for a program created to analyze linear elastic problems, solved by FEM using 2-D cartesian meshes independent of geometry. Evaluating the results obtained, the theoretical bases available in the literature on the calculation of sensitivities have been adapted properly to an environment for which they were not developed in the beginning, thus overcoming the requirements arising from the use of cartesian meshes independent of the geometry and, on the other hand, various methods to generate robust and efficient velocity fields have been implemented as well. To evaluate the quality of the calculations we have implemented an error estimator based on SPR techniques. In general we can say that among the velocity field evaluation techniques analyzed, which provides better results in problems with a smooth solution is the physical approach of FE. The creation of the velocity field using this technique requires solving a problem with the same size of the original problem and that is usually done by a direct solver for small size problems but for large size problems the use of iterative procedures could be interesting.

ACKNOWLEDGEMENTS

With the support from Ministerio de Economía y Competitividad of Spain (DPI2010-20542), FPI program (BES-2011-044080), FPU program (AP-2008-01086) Generalitat Valenciana (PROMETEO/2012/023), EU project INSIST (FP7-PEOPLE-2011-ITN) and Universitat Politècnica de València.

REFERENCES

- [1] T. Strouboulis, K. Copps and I. Babuška. *The Generalized Finite Element Method: an Example of its Implementation and Illustration of its Performance*. Int. Journal for Num. Methods in Eng., (2000) 47:1401-1417.

- [2] N. Moës, J. Dolbow and T. Belytschko. *A Finite Element Method for Crack Growth without Remeshing*. Int. Journal for Num. Methods in Eng., (1999) 46:131-150.
- [3] D.F. Rogers. *An Introduction to NURBS with Historical Perspective*. Morgan Kaufmann, (2001).
- [4] L. Piegl and W. Tiller. *The NURBS Book*. Springer, (1997).
- [5] K. Qin. *General Matrix Representations for B-splines*. The Visual Computer, (2000) 16:1-13.
- [6] W.J. Gordon and C.A. Hall. *Construction of a Curvilinear Coordinate Systems and Applications to Mesh Generation*. Int. Journal for Num. Methods in Eng., (1973) 7:461-477.
- [7] K.K. Choi and K.H. Chang. *A Study of Design Velocity Field Computation for Shape Optimal Design*. Finite Elements in Analysis and Design, (1994) 15:317-341.
- [8] D. Belegundu, S. Zhang, Y. Manicka and R. Salagame. *The Natural Approach for Shape Optimization with Mesh Distortion Control*. Penn State University Report. College of Engineering. University Park, Pennsylvania, (1991).
- [9] O.C. Zienkiewicz, J.Z. Zhu. *A Simple Error Estimation and Adaptive Procedure for Practical Engineering Analysis*. Int. Journal for Num. Methods in Eng., (1987) 24:337-357.
- [10] O.C. Zienkiewicz, J.Z. Zhu. *The Superconvergent Patch Recovery and a-Posteriori Error Estimates. Part I: The Recovery Technique*. Int. Journal for Num. Methods in Eng., (1992) 33:1331-1364.
- [11] J.J. Ródenas, M. Tur, F.J. Fuenmayor and A. Vercher. *Improvement of the Superconvergent Patch Recovery Technique by the Use of Constraint Equations: The SPR-C Technique*. Int. Journal for Num. Methods in Eng., (2007) 70:705-727.
- [12] F.J. Fuenmayor, J.L. Oliver and J.J. Ródenas. *Extension of the Zienkiewicz-Zhu Error Estimator to Shape Sensitivity Analysis*. Int. Journal for Num. Methods in Eng., (1997) 40:1413-1433.
- [13] J.J. Ródenas, F.J. Fuenmayor and J.E. Tarancón. *A Numerical Methodology to Assess the Quality of the Design Velocity Field Computation Methods in Shape Sensitivity Analysis*. Int. Journal for Num. Methods in Eng., (2003) 59:1725-1747.